DOI: 10.21062/mft.2023.052 http://www.journalmt.com

High Temperature Protective Coatings for Aeroengine Applications

Jakub Jopek (0009-0003-5856-3578), Magdalena Mokrzycka (0000-0002-3153-0990), Marek Góral (0000-0002-7058-510X)*, Barbara Koscielniak (0000-0002-1683-0354), Kamil Ochal (0000-0002-0708-2542), Marcin Drajewicz (0000-0002-9600-6938)
Research and Development Laboratory for Aerospace Materials, Rzeszow University of Technology, Powstancow Warszawy 12, 35-959 Rzeszow, Poland. Corresponding author * e-mail: mgoral@prz.edu.pl

Nickel superalloys are the main materials used in manufacturing of turbine blades and vanes in aerospace industry. They works is extremely high temperature in a corrosive environment (oxidation, hot corrosion) and undergo several different thermo-mechanical loads. Aluminide coatings are the main method of protection of the surface of nickel superalloys against exhaust gasses environment in jet engine. In presented article the microstructural characterization of aluminide coatings produced using two industrial methods (pack cementation and out of pack) was conducted. The commercially available powders manufactured by Oerlikon-Metco were used in aluminizing process using industrial Bernex BPX Pro 325S CVD system. The Mar M247 was used as a base material. Amount of activator and pure aluminum had a noticeable effect on the total thickness of obtained layers. Both samples with increased activator and pure aluminum content formed 5 to 11.5 x thicker aluminide coatings in comparison to other sample, which was aluminized using an Al-Co powder as aluminum source. Further investigations are needed to specify precise phase composition of analyzed coatings.

Keywords: aluminide coatings, turbine blades, MAR M247, CVD

1 Introduction

Contemporary aviation industry is mainly focused on increasing gas turbine efficiency, which is inextricably linked with the process of raising temperature of hot gases in combustor chamber. One of the factors that hasten this increase are materials and production technologies of high- pressure turbine blades. They work under extremely high temperature in a corrosive environment and undergo several different loads. It creates the problem of proper material selection and a method of its protection against several degradation mechanisms that can occur in hot section of aircraft gas turbine. Only nickel-based superalloys can withstand such a harsh environment for a long time, and they are in use since 1950s. One of them is polycrystalline Mar M-247 alloy, which was developed in 1970s. It possesses excellent oxidation resistance and high creep strength at elevated temperatures. After casting its microstructure is composed of: γ'-Ni_3(Al, Ti) strengthening phase (62 vol. %), γ matrix, γ/γ' eutectic and carbides [1]. Although they offer outstanding mechanical properties in operating temperatures, they are very susceptible to oxidation which causes its unacceptable degradation, drastically limiting components lifetime [2,3]. That is why aluminide protective coatings have been developed [4-8].

Aluminide coatings can be divided into two main categories based on the aluminum activity of the pack [6]. High activity low temperature process (HALT) takes place at 700 – 900 °C. Coating is formed by a predominant inward diffusion of aluminum atoms into the nickel substrate. The resulting microstructure consists of an external δ-Ni_2Al_3 phase and internal β-NiAl with dispersed MC and $M_{23}C_6$ carbides in both layers. Because δ-Ni_2Al_3 is more brittle and oxidizable than β -NiAl, heat treatment is applied at 1050 – 1100 °C. After that, microstructure has three visible layers. Inner layers is composed by columnar grains of β-NiAl phase with dispersed MC, $M_{23}C_6$ carbides and σ (Cr, Mo, Co) phase, while the outer layer comprises equiaxed β-NiAl grains and substrate carbides. Middle layer is single-phase β-NiAl. Low activity high temperature process (LAHT) is conducted at 1050 – 1100 °C, when aluminum activity is low. Its kinetics is controlled by outward diffusion of nickel atoms and it has two zones. The inner zone is similar to that observed in HALT process and consists of β-NiAl, MC, $M_{23}C_6$ carbides and σ phase. The outer zone comprises β-NiAl phase with substrate alloying elements dissolved [5,7,9-12]. In order to obtain optimal aluminide coatings on superalloy substrates, many methods of aluminization were developed: pack cementation, gas methods (vapor phase aluminizing-VPA and above the pack), chemical vapor deposition (CVD) and slurry.

Among many available methods, pack cementation attracted the most attention of industry thanks to its simplicity and low cost [9,13-16]. Thoroughly cleaned and dried samples are immersed in powder mixture and placed in a sealed heat-resistant steel box. Powder mixture contains aluminum source (aluminum or its alloy), activator (fluoride salt such as NaF) and filler (e.g. Al_2O_3 preventing mixture from sintering). Upon heating the pack to desired temperature, activator volatilizes and reacts with metal powder to form volatile aluminum compounds which diffuse towards the alloy surface. Subsequently, aluminum halides react with the alloy and release aluminum atoms. Diffusion reactions take place after which aluminides are formed. As a result, aluminum activity on the metallic substrate is lowered, allowing further continuation of the process [9,14,15]. Although this method has many advantages, it is unsuitable for the coating of complex cooling channels. Difficulties arise during feeding such channels and removing of mixture after aluminization [5]. Furthermore, powder particles might be built in the coating, lowering its functional properties [12]. It forces additional machining to regain proper coating structure. That is why more frequently engineers choose processes that do not involve any physical contact between powder mixture and parts to be coated.

One of such methods is CVD where samples and aluminum source are completely separated from each other. Although being very complex, CVD has gained much attention because of the possibility to widely control process parameters, thus obtaining desired structures of aluminized layers on different substrates. In an external generator, at a temperature of 300 °C, HCl gases pass through aluminum granules to form aluminum chlorides. Then they are being heated to approx. 1000 °C and transported to the main reactor. Upon their diffusion to the parts surface, $AlCl_x$ vapor react with nickel to form β-NiAl coating. Outer generator enables to precisely control flow rate of gases, allowing to obtain eligible aluminum activity inside main reactor [12,17]. Chemistry of the coating can be further changed by the incorporation of additional elements (such as Hf, Y, Zr) at precise level [18]. Coatings produced by this method have exceptional quality and may be relatively easily modified for better corrosion resistance. However, CVD has some serious drawbacks arising from its complexity. This method is neither cheap, nor simple and requires specialized equipment to conduct it successfully. In order to meet specified quality requirements of aluminum coatings at the lowest cost possible, another method is often chosen.

Gas methods (VPA and above the pack) merge the features of CVD and pack cementation process. They are still relatively cheap and do not require sophisticated apparatus, while providing good surface quality of coated samples. Moreover, they allow a proper coating of internal cooling channels of high-pressure turbine blades without insertion of powder particles inside them. Coated parts are placed in the retort furnace, while being physically separated from the pack or granules (in case of VPA method). Aluminizing begins with the formation of aluminum subchlorides, which are being transported to the substrate by gaseous diffusion. Afterwards, reactions resulting in the deposition of aluminum on the parts surface take pace. In this moment, aluminum diffuses into the substrate to form intermetallic phases, whilst reaction products diffuse back to the reactor. Solid-phase diffusion and vapor transport are the slowest stages in the whole process, hence they control kinetics of coating growth [12,17,19].

In our previous research the two aluminizing methods were analyzed – out of pack [20] as well as CVD [21]. In paper [17] the initial comparative study of aluminide coatings produced by slurry, pack cementation, out of pack and CVD methods in the aspects of their thickness, Al content and oxidation resistance was conducted.

2 Experimental

Mar M-247 superalloy (Tab. 1) was aluminized and alumino-silicized in different conditions (Tab 2). Supplied bar was cut into specimens, 20 mm in diameter and 4 mm in height, grinded and degreased in isopropanol. All processes were conducted using industrial CVD system Bernex 325S produced by Ion Bond (Switzerland). In the processes, retort low-pressure furnace with Ar-flow line installed in this device was used. All processes were conducted under pressure 100 mbar in argon atmosphere with a flow 0.6 LPM (Normal litres per minute). Pack aluminizing was done for processes signed as M1, M3, M4, M5. Different powder mixtures and temperature were used (Tab. 2). Samples were immersed in powder mixture and placed in specially designed refractory container.Alumino-silicizing out of pack was carried out by placing samples (M2) on holders above pack mixture. Pack contained 80% AMDRY 356 as an inert filler, 10% Al + 10% Si as the saturate sources and 2% NH_4F as activator. The diffusion treatment was conducted at 950 °C for 4 h (Tab. 2). The microstructural investigation of obtained aluminide coating was conducted using Hitachi S-3400 Scanning Electron Microscope equipped with EDX detector (Thermo). Coatings thickness was measured using ImageJ software.

Tab. 1 *Chemical composition of Mar M-247 alloy*

Alloy	Element content (wt.%)												
	Ni	Co	Cr	Mo	Al	Ti	Zr	C	Fe	B	W	Ta	Hf
Mar M-247	Bal.	10.0	8.6	0.8	5.6	1.0	0.06	0.16	0.2	0.020	10.0	3.0	1.5

Tab. 2 *Aluminizing conditions for M1 – M5 samples; process time: 4 h*

Process	Method	T [°C]	Powder mixture
M1	Pack cementation	950	90% AMDRY 356+ 10% CODEP + 2% NH_4Cl
M2	Out of pack	950	80% AMDRY 356 + 10% Al + 10% Si + 2% NH_4F
M3	Pack cementation	1040	100% AMDRY 353+ 2% NH_4Cl
M4	Pack cementation	1040	50% AMDRY 353 + 50% AMDRY 356 + 5% NH_4Cl
M5	Pack cementation	1040	80% AMDRY 356 + 20% Al + 2% NH_4Cl
Composition of AMDRY 356: 100 wt. % Al_2O_3 Composition of AMDRY 353: 46.5 wt. % Co + 53.5 wt.% Al			

3 Results and discussion

3.1 M1 Coating

First coating was obtained via pack cementation M1 process in 950°C/4h (Tab 2). It consists of two visible and uniform layers with total thickness of 17 μm (Fig. 2.) The outer layer is 10.1 (+/- 1.1 μm) thick, while the interlayer (inner) 6.9 (+/- 0.4 μm). Interlayer accounts for nearly a half of the whole coating thickness, which suggests that the process featured mostly outward nickel diffusion. Sitek et al. [22] aluminized In100 alloy in the same conditions by CVD method obtaining 11 μm thick coating: 5 μm outer and 6 μm interlayer. β-NiAl phase was identified and in the interlayer increased amount of chromium, titanium and carbon was observed. The same conditions were used to aluminize In 713C alloy by CVD method and a coating of 17 μm total thickness was obtained. It consisted of two visible layers: outer (8 μm) and inner (9 μm) [23]. Bozza et al. [24] aluminized CM-247 LC alloy, a derivative of Mar M247, in a pack mixture (10 wt. % CoAl + 0.3 wt. % AlF_3 + 89.7 wt. % Al_2O_3) in 950°C for 4 h. Hardness measurements confirmed the presence of δ-Ni_2Al_3 phase with large inclusions of titanium, tungsten and tantalum carbides. No interdiffusion layer was found. Formation mechanism of aluminized layer was proposed by an inward diffusion of aluminum atoms. In M1 sample, near the surface, aluminum content is maximum (26.8 wt. %), whilst nickel is in amount of 50 – 53 wt. % (Fig. 1).

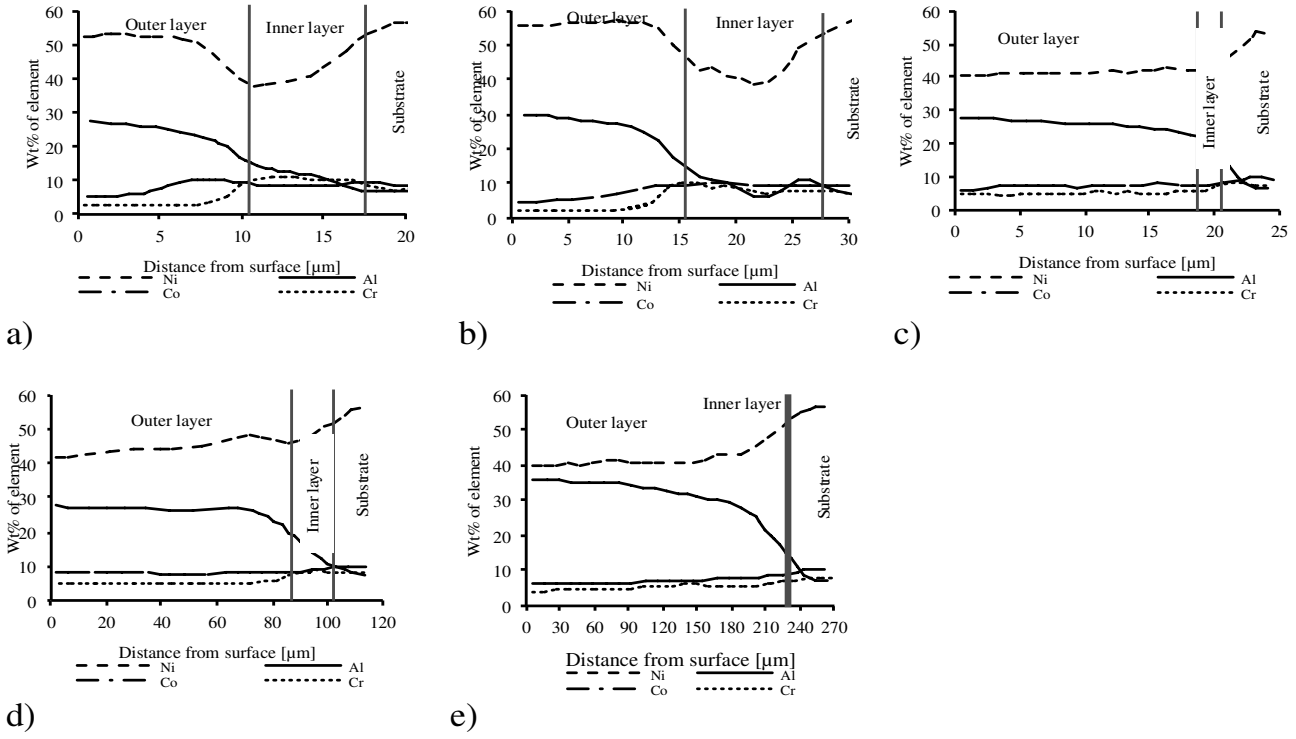

Fig. 1 *Cocnentration of Ni, Al, Co, Cr in the aluminide layers obtained on Mar M-247 alloy for different aluminide conditions: (a) M1, (b) M2, (c) M3, (d) M4, (e) M5 (wt. %); The red lines separate the additive layer, the diffusion layer and the substrate*

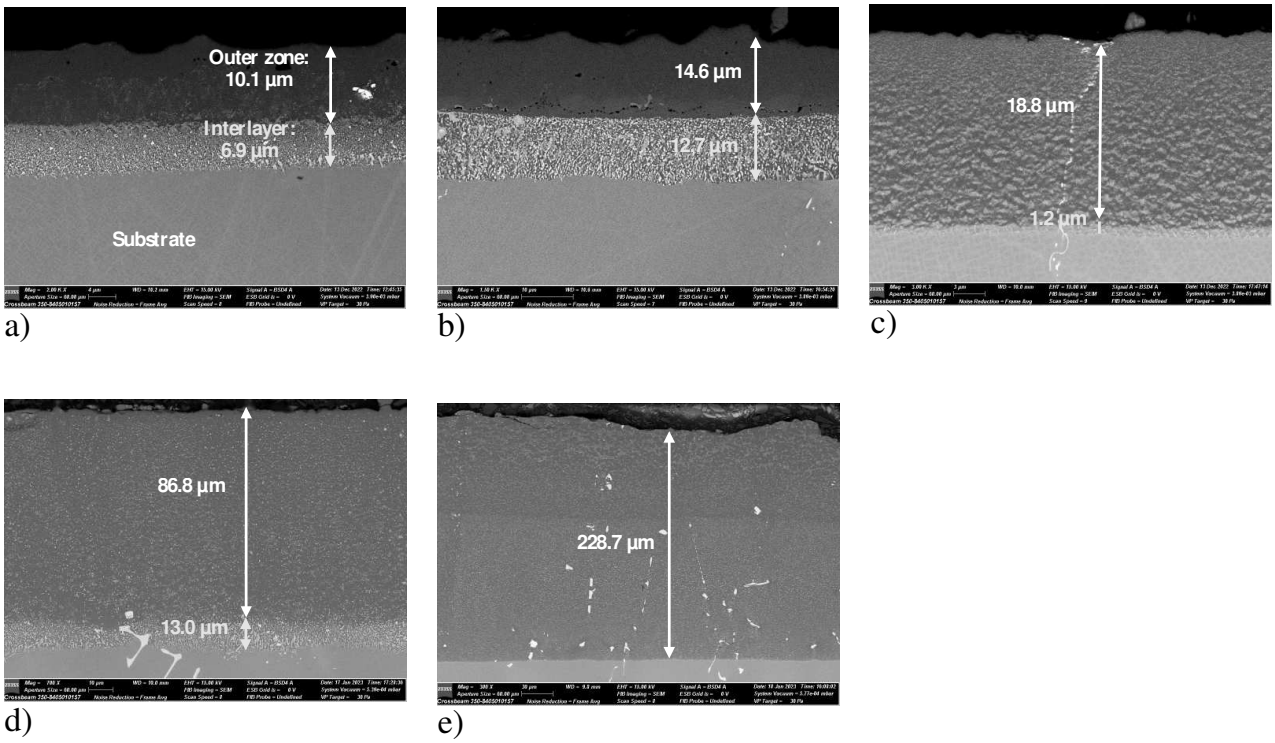

Fig. 2 *Cross-sectional back-scattered electron micrographs of as-prepared coatings on Mar M-247 alloy using different methods and under different conditions: a) M1, b) M2, c) M3, d) M4, e) M5 with marked thickness measurement of outer layer (white line) and inner layer(yellow line)*

Tab. 3 *Thickness of aluminide layers obtained on Mar M-247 alloy by different methods*

Sample	Thickness of aluminide layers zone [µm]		
	Outer	Inner	Sum
M1	10.1	6.9	17.0
M2	14.6	12.7	27.3
M3	18.8	1.2	20.0
M4	86.8	13.0	99.8
M5	228.7	2.1	230.8

Some bright phases are visible- these are probably Ni_3Al or σ-Cr phases (Fig. 2a). According to the Ni-Al equilibrium diagram [25], this might be β-NiAl phase with alloying elements dissolved in it. Spherical dark areas are probably Al_2O_3 filler granules built in the surface as a result of a physical contact between powder mixture and sample during coating (Fig. 2,3). In the interlayer, aluminum content decreases (20 – 8 wt. %) to reach its minimum at the distance of 20 µm: 7.2 wt. % (Fig. 1), just beneath the interlayer. Nickel content is minimum here: 38 – 44 wt. %. Intermetallic phases that may be there are β -NiAl (dark grey) and Ni_3Al (light grey) [25]. On the other hand, content of some elements (W, Ta, Cr, Ti) reach its peak in there: 18 wt.% W, 7.6 wt. % Ta, 10 .wt% Cr, 1.5 wt. % Ti. This indicates the presence of many precipitates, further confirmed by the SEM mapping analysis (Fig. 3) and BSE images (Fig. 2a). They were formed during aluminizing. Before the coating process, fully heat-treated Mar M-247 alloy has a microstructure mostly composed of γ matrix, γ' strengthening phase ($Ni_3(Al$, Ti)) and carbides [26,27]. During aluminizing, nickel atoms diffuse to the sub-surface areas, while aluminum diffuses in the opposite direction. Cr-, Ta-, Ti- and W- atoms diffusion rates are very low in such conditions, so they are practically immobile. Interlayer is formed as a result of a partial depletion of nickel atoms that diffuse towards surface, while Cr, Ta, W, Ti form their own phases [13,22]. Chemical composition of areas in different shades of gray (Tab. 4, spectrum 03 - 04) as well as elongated precipitates was analyzed (Tab. 4, spectrum 01 - 02). In its upper part, this phases contained hafnium and more tantalum, whereas its elongated bottom part had more tungsten and chromium. They might be identified as MC carbides consisting of two parts: the upper one could be (Ta, W, Hf)C and the bottom one (W, Ta)C. Similar results were obtained in paper [28], where greater amounts of hafnium was observed in MC carbides heads. There are also a few small hafnium-rich areas in the interlayer and beneath it (Fig. 3). They may be HfC carbides, because this phases are very

stable and hafnium is a carbide-forming element [29]. Numerous phases, visible at the coating/substrate interface, are bigger than those above them. They have a shape close to columnar which reflects the direction of nickel and aluminum diffusion. Big, irregular phases were also present across the coating. As they contain carbide-formers it is probable that those were undissolved MC (M = W, Ta, Hf, Ti,) primary carbides (Fig. 2a) [22]. Aluminized layers on Mar M247 alloy were also produced via a slurry method using Ceral 10 suspension [17]. It consists of Al and Si powder with an inorganic binder. After 4 h at 950°C, thickness of coating reached 60 μm and the aluminum amount was 26 wt. %.

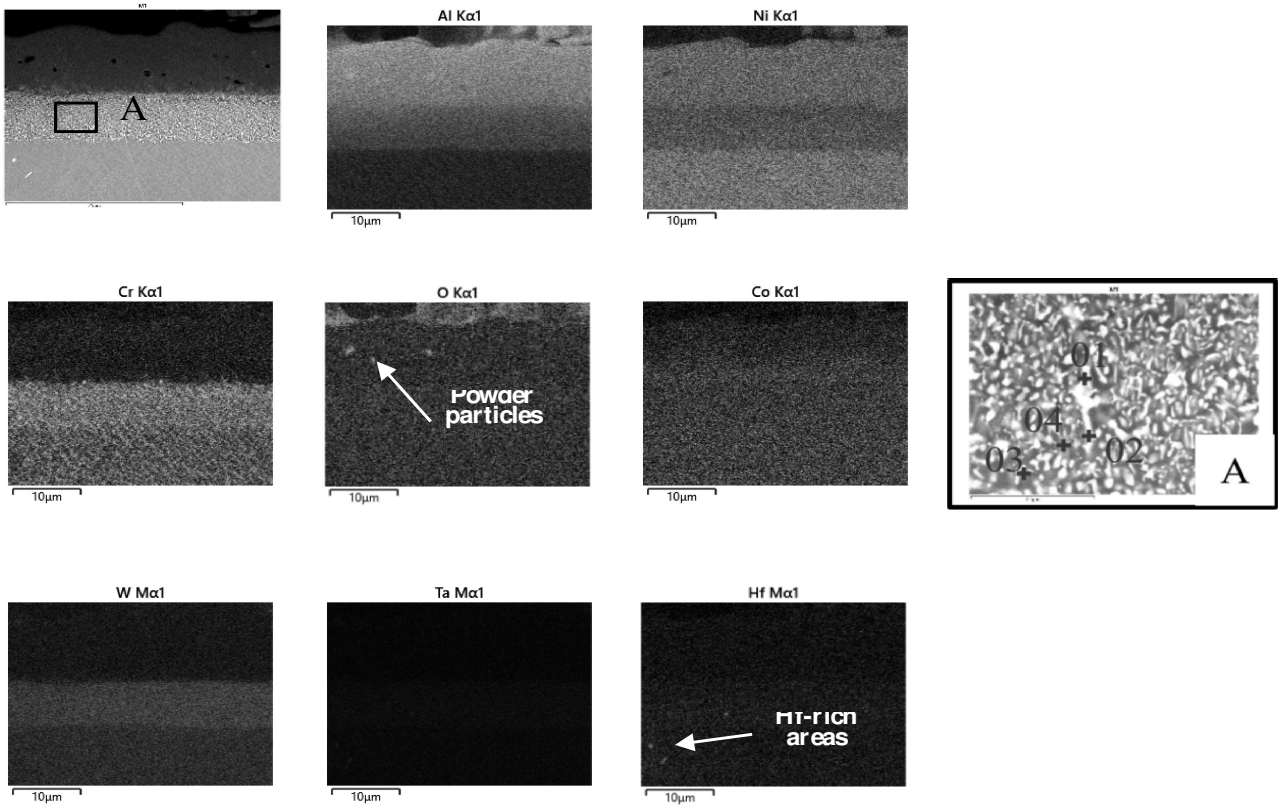

Fig. 3 *Elemental mapping of elements in M1 nickel-based superalloy*

Tab. 4 *Point analysis of enlarged area form Fig. 3*

Area	Element content (wt.%)								
	Ni	Al	Co	Cr	Ti	Ta	W	Hf	Mo
01	31.60	10.06	6.47	7.55	2.33	17.82	12.36	8.94	0.81
02	35.77	10.74	9.08	11.13	1.41	9.76	18.55	-	1.47
03	45.19	13.10	8.20	9.30	1.99	8.08	11.22	-	0.80
04	38.98	11.91	8.09	14.56	1.79	7.73	13.87	-	1.01

3.2 M2 coating

Aluminized layers modified with silicon are often used to improve oxidation resistance of Ni-based superalloys [5,7,30,31]. Coating on Mar M-247 alloy was obtained by out of pack method (950°C/4h) using powder mixture that contained aluminum and silicon (Tab. 2). It has a total thickness of 27.3 μm (Tab. 3): the outer layer is 14.6 (+/-1.8 μm) thick and the interlayer 12.7 (+/-1.1 μm) thick (Fig. 2b). According to ref. [13], to obtain aluminized coatings alloyed with silicon, Al/Si ratio in the saturating mixture must be within the range of 1:9 – 9:1. If the silicon content exceeds 50%, thickening of the coating will be observed. In this case, Al/Si ratio equals 1:1 and indeed resulting coating was thicker in comparison to M1 sample aluminized in the same conditions (Tab 3.). Its structure suggests that it was formed by a predominant outward diffusion of nickel atoms. In the outer layer aluminum content is in the range of 30 – 25 wt. % (Fig. 1), while nickel is in amount of 53 – 56 wt. %. The intermetallic aluminide phase present here may be β-NiAl [25]. Linear analysis shown that silicon mass volume in this area is steady: ~3 wt. %. Similar

results presented Wu et al. [32] as they identified 3.4 – 4.0 wt. % Si in the outer and inner part of aluminized layer prepared by pack cementation process (10wt% Al + 10 wt. % Si + 75 wt. % Al_2O_3 + 5 wt. % NaF) on the IC20 superalloy substrate (1100°C/1.5h). Moreover, clear cobalt gradient concentration is visible (Fig. 1b, 4 and). Concentration of chromium in the outer layer is very low (less than 2wt%), due to its limited solubility in β-NiAl phase (Fig. 1b) [33]. A chain of micrometer globular areas in the lower part of outer layer is visible (Fig. 2b). Some of them have increased concentration of oxygen and chromium (Fig. 4, marked with yellow arrow), while the others do not (Fig. 4, marked with red arrow). Those without a clear concentration of any element might be Kirkendall pores. Such defects form due to unbalanced nickel flux towards surface which can lead to a deficiency of atoms at the outer/inner zone interface and formation of large voids [34] Characteristic feature of interlayer is increased amount of some alloying elements that reach their maximum in there: 20 wt. % W, 9 wt. % Ta, 10 wt. % Cr. Other metals (Hf, Mo, Si, Ti) also reach their peaks in the interlayer. Changes in element contents derive from the process of "pushing back" their atoms during the growth of β-NiAl grains [35]. In the interlayer and substrate there are many bright spherical precipitates with a diameter of ca. 3 μm distributed in the interlayer and the upper part of substrate (Fig. 2b). Mapping of the coating and linear analysis showed that there is no nickel, aluminum and cobalt in these areas. On the other hand, strong concentration of W, Ta, Hf, Ti and Si was observed (Fig. 4). Silicon comes from the powder mixture (Tab. 2)(and it was co-deposited during the process. According to [36] it might form silicates with: W, Ta, Hf and Ti. The analysis revealed that hafnium concentrated only in these precipitates (Fig. 4). Chromium-rich phases are dispersed throughout the outer and interlayer (Fig. 4). They are smaller than carbides and irregular in shape. Their occurrence derives from a restrained solubility of chromium in β -NiAl phase (~10 at. % at 1050°C), which is significantly decreasing with decreasing temperature [37] Nickel content is minimum here (38 wt. %), whereas the aluminum is steadily lowering to obtain the value of 7.2 wt. % at the distance of 30 μm(Fig. 1). Main intermetallic phases from the Ni-Al equilibrium diagram are probably: β -NiAl and Ni_3Al [25]. Tu et al. [38] prepared Al-Si coatings on the substrate of IC211 superalloy by pack cementation method with a pack composition: 10 wt. % Al + 2 wt. % Si + 5 wt. % NaF + 83 wt. % Al_2O_3. After aluminizing for 1.5 h in 1000°C they obtained a double-layer coating, ~150 μm thick, with a homogeneous concentration of ~1 at. % Si.

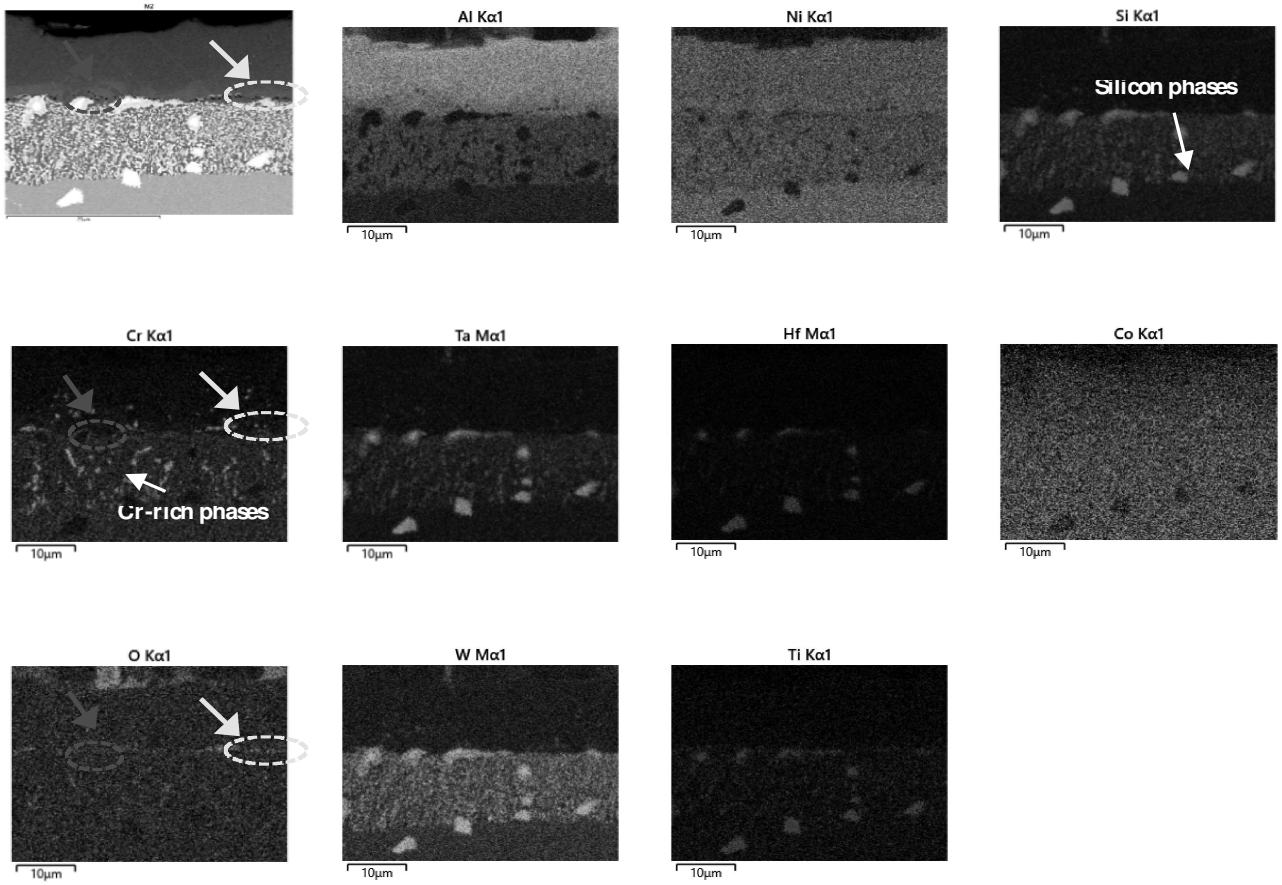

Fig. 4 *Elemental mapping of elements in M2 nickel-based superalloy*

3.3 M3 coating

Two layers are visible on the substrate of Mar M-247 alloy aluminized by pack cementation process in 1040°C/4h (Fig. 2c): outer 18.8 (+/- 0.4 μm) thick and interlayer 1.2 (+/- 0.1 μm) (Tab. 3). No defects (pores, particle inclusions) are visible. Powder mixture used in this process (100% AMDRY 353) consists of aluminum (53.5 wt. %) and cobalt (46.5 wt. %). According to paper [13], presence of second alloying element in an aluminum source (e.g. Fe, Cr or Co) lowers its activity, decreasing thickness of the coating. Therefore the M3 coating is much thinner (20 μm) in comparison to M4 – M5 coatings (99.8 and 228.7 μm) obtained in the same conditions (Tab. 3). Aluminum content is gradually decreasing in the range of 28 – 24 wt. %, while nickel increasing (40 – 43 wt. %). High temperature (1040°C) and lowered aluminum activity were enough factors to inhibit the formation of δ-Ni_2Al_3 phase. Instead, highly-saturated with aluminum and alloying elements (~30 wt. %) β -NiAl phase was probably formed. On this basis, we might assume that the coating was produced via the inward diffusion of aluminum. The coating itself is not featureless and is composed of two main components forming a specific mélange: dark-gray matrix with light-gray feathery phases (Fig. 2c). SEM microanalysis revealed the presence of a few micrometer phases forming a chain across the coating in the direction perpendicular to its surface (Fig. 2c). W, Ta, Ti and C were detected. Observed phases are probably primary MC or $M_{23}C_6$ carbides [22,39] The amount of Cr (5 – 8 wt. %), Co (6 – 9.5 wt. %) and W (10 – 15 wt. %) is gradually increasing to reach their peaks at the coating/substrate interface. Chromium, tantalum and tungsten are a bit more concentrated in the narrow interlayer, while the content of aluminum is drastically lowering in there. This was confirmed by mapping analysis (Fig. 5, white arrow). Góral et al. [17] aluminized Mar M247 alloy using different techniques and varying process parameters. All of the most frequently utilized methods were investigated. After the VPA (1020°C/4h) with a powder mixture containing 44 wt. % Al, a 50 μm coating with 33 wt. % Al was obtained. The pack cementation and out of pack methods based on the same powder mixture: 30 wt. % Al + 1 wt. % AlF_3 + bal. Al_2O_3. Processes were conducted in 1000°C for 4 h. First method allowed to produce a 70 μm layer containing 29 wt. % Al, while the latter a 140 μm coating with 33 wt. % Al.

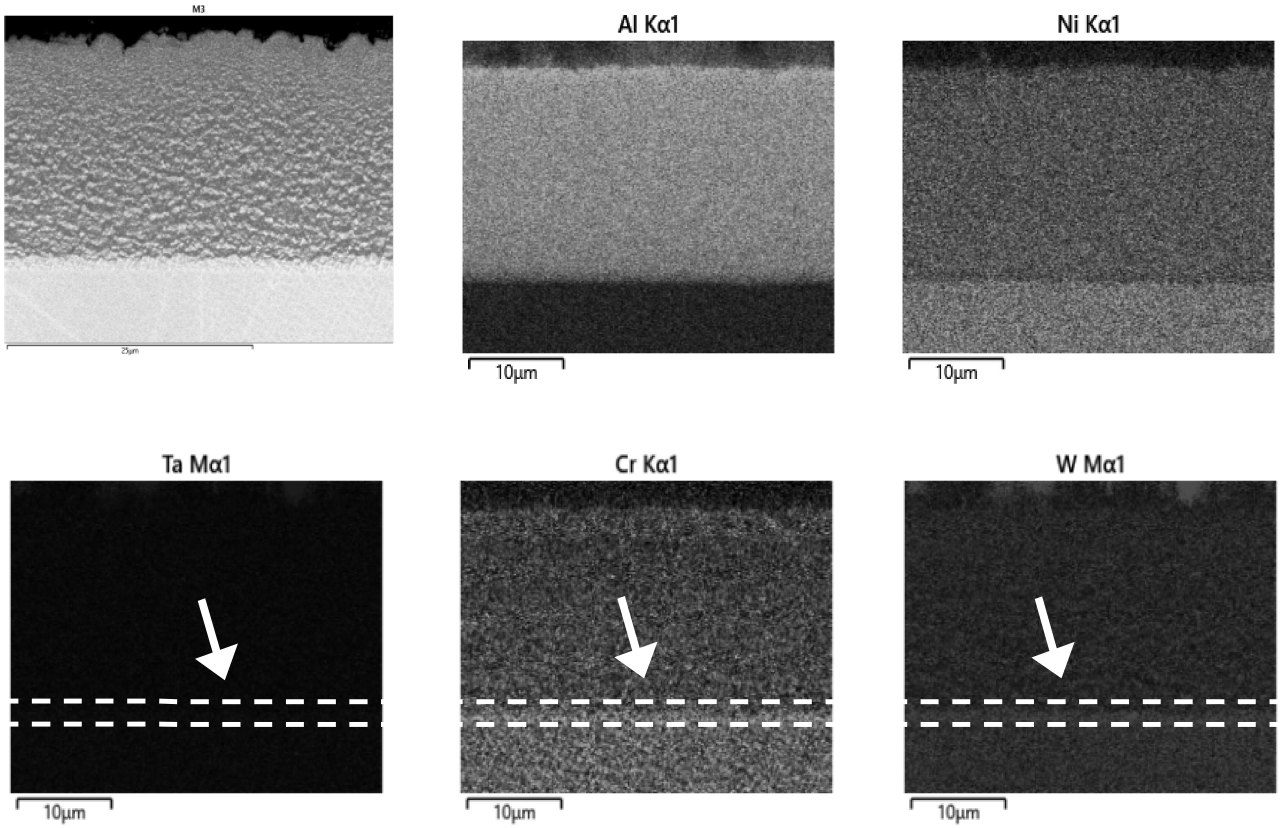

Fig. 5 *Elemental mapping of elements in M3 nickel-based superalloy*

3.4 M4 Coating

M4 coating was obtained via pack cementation aluminizing in 1040°C/4h. The use of powder mixture containing 50% AMDRY 353 and 50% AMDRY 356 (Tab 2) resulted in a formation of two-zone uniform aluminized layer: outer (86.8 +/-1.9 μm) and inner (13.0 +/-1.3 μm). No defects were observed (Fig. 2d). Such a thick coating can be attributed to a very high

amount of activator used (5% NH_4Cl, for other samples it was 2% NH_4Cl) which strongly affects resulting coating thickness [13]. Outer layer accounts for almost 90% of whole coating thickness, which suggests that the coating was formed by a predominant nickel outward diffusion. The amount of nickel in this zone is within the range: 42 – 48 wt. %, while aluminum: 28 – 20 wt. %. Moreover, there is approx. 29 wt. % of other alloying elements. Outer layer is composed of two main phases with bright, small spherical precipitates rich in Cr, W and Ta (Fig. 7). On the other hand, gray matrix contains ca. 55 wt. % Ni and 29 wt. % Al which implies the existence of β -NiAl phase (Tab 5, spectrum 08 in the bottom part of outer zone). Interlayer comprises a dark-gray matrix and numerous precipitates in different shapes of grey (Fig. 2d). EDS mapping analysis showed, that some of them are rich in chromium and others in: W, Ta, Hf (Fig. 6,7) Elemental mapping and point analysis showed that in the aluminized layer all hafnium concentrated in carbides (Tab. 5, Fig. 7) Interlayer is slightly depleted of nickel, due to its little outward diffusion during aluminizing (Fig. 1d). Also, clear aluminum gradient is visible (Fig. 1d, 6). Maximum concentration in this zone reach following elements: Cr (9 wt. %), W (12.5 wt. %), Ti (1.3 wt. %). Two types of carbides can be found in Mar M247 alloy [1, 39-41] First of them are primary MC (M = Ta, Ti, Hf, W) carbides, coarse and elongated, with a diameter of 2 – 10 μm. These carbides were found to have a complex composition with different amounts of carbide-formers [39] There are also secondary (0.2 – 0.8 μm in diameter) Cr-rich $M_{23}C_6$ carbides, which precipitate along grain boundaries forming thin networks [1]. As the bright phases presented in (Fig. 6,7) are coarse and elongated and contain fair amount of tantalum (Tab. 5, spectrum 05 and 06), it is probable that they are (Ta, W, Ti, Hf)C carbides. Szczotok et al. [39] reported the occurrence of similar carbides with almost the same chemical composition in casted MAR M-247 alloy after thermal cycling. Jonšta et al. [42] also identified (Ta, Hf, W, Ti)C carbides in as-casted condition. Their presence in the outer layer further confirms its formation mechanism.

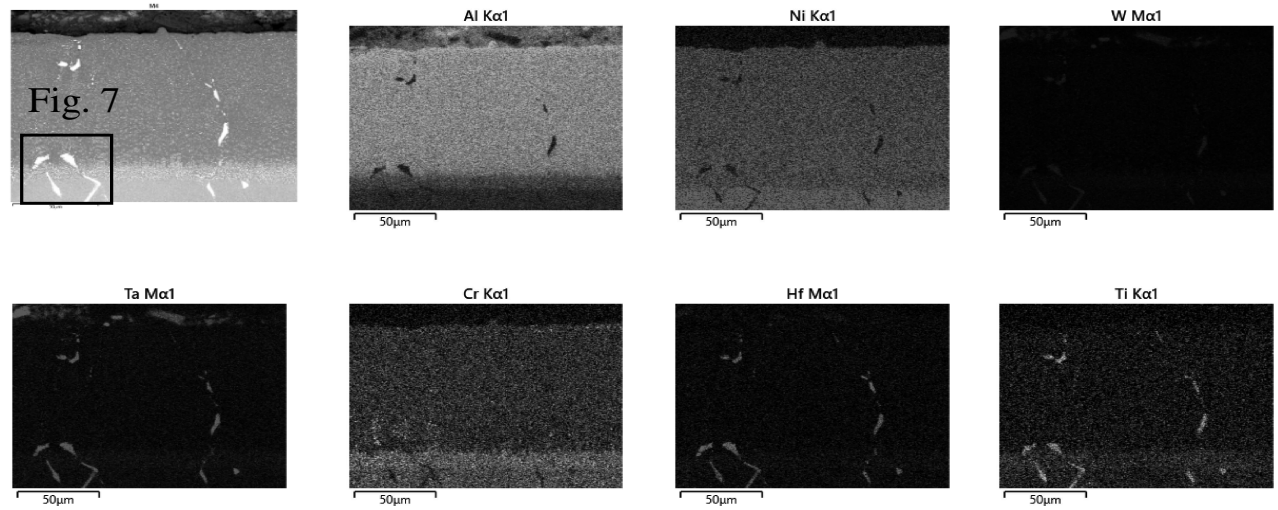

Fig. 6 *Elemental mapping of elements in M4 nickel-based superalloy*

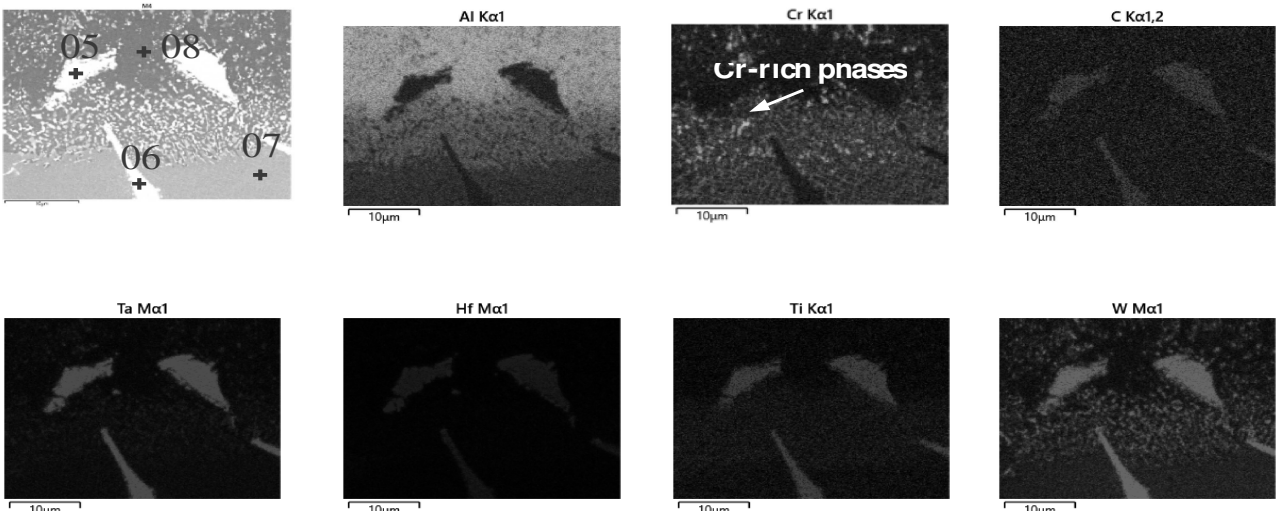

Fig. 7 *Elemental mapping of elements in M4 nickel-based superalloy. Enlarged area form Fig. 6*

Tab. 5 *Point analysis of enlarged area form Fig. 7. Weight % of elements in analyzed points*

Spectrum Label	Element content (wt.%)								
	Ni	Al	Co	Cr	Ti	Ta	W	Hf	Mo
05	14.56	3.13	2.34	2.43	7.67	46.19	13.39	9.33	0.95
06	15.65	2.47	2.92	3.16	8.09	42.68	18.42	5.36	1.24
07	57.87	8.03	8.72	6.37	1.10	6.04	11.59	-	0.29
08	54.50	29.44	8.11	4.23	0.4	-	3.33	-	-

3.5 M5 coating

Mar M247 alloy was also pack aluminized in 1040°C/4h with a use of mixture containing 80% AMDRY 356 and 20% Al. Among all variation of powder mixture, M5 had the most pure aluminum as a source (20 wt. %). Thus, resulting monolayer coating was the thickest among all obtained in the same conditions (Tab. 2): 228.7 +/-7.8 μm (outer layer) and 2.1 +/-0.4 μm (interlayer). According to ref. [13], increased amount of aluminum powder results in more available aluminum atoms that can saturate substrate material. Aluminum activity is then higher and the coating becomes thicker. Due to high activity of powder mixture, only a very narrow interlayer was formed (Fig. 2e) and coating was created by an inward diffusion of aluminum atoms. In its upper part, coating is composed of three main constituents (Fig. 10b). Spectrum 14 represents chemical composition of big, irregular phases – they are rich in chromium, tungsten and aluminum (Tab. 6). Matrix is represented by spectrum 15 and its chemical composition suggests the presence of β-NiAl phase. Spectrum 16 shows chemical composition of small, dense phases that are rich in tantalum (11.74 wt. %) and tungsten (12.61 wt. %). In the bottom part of aluminized layer there are also three different phases (Fig. 10a). Chromium and tungsten are concentrated in dense phases with a diameter of ~1 μm (Tab. 6, spectrum 11 and 12) dispersed in the matrix, which have a composition typical for β -NiAl phase (Tab. 6 spectrum 13). There are also numerous, nanometer-size bright precipitates- they were not analyzed in this paper. A slight gradient of aluminum concentration is visible from the maximum content of 36 wt. % just beneath the surface. Nickel is within the range: 40 – 45 wt. % and no more than 28 wt. % of alloying elements can be found in the coating. A narrow interlayer can be observed with increased W, Ta, Hf, Ti and Cr concentration (Fig. 9, white arrows). Coarse and elongated phases are dispersed throughout the coating and substrate (Fig. 8). Mapping analysis of enlarged area (Fig. 9) as well as point analysis (Tab. 6, spectrum 09 - 10) revealed that they comprise carbon and carbide-formers, so they could be identified as primary (Ta, W, Hf, Ti)C carbides [39]. Substrate material contains ~1.5 wt. % Hf (Tab. 1). In the aluminized layers it concentrates entirely in MC carbides with "Chinese script" structure [28,29,42], as no hafnium was identified in other places (Tab. 6). Eslami et al. [43] conducted gas phase aluminizing of GTD-111 nickel-based superalloy using a mixture with different amounts of aluminum and activator (1040°C/4h). With the use of 10 – 30 wt. % Al, 5 wt. % NH_4Cl and balance Al_2O_3, they obtained 22 – 30 μm coatings.

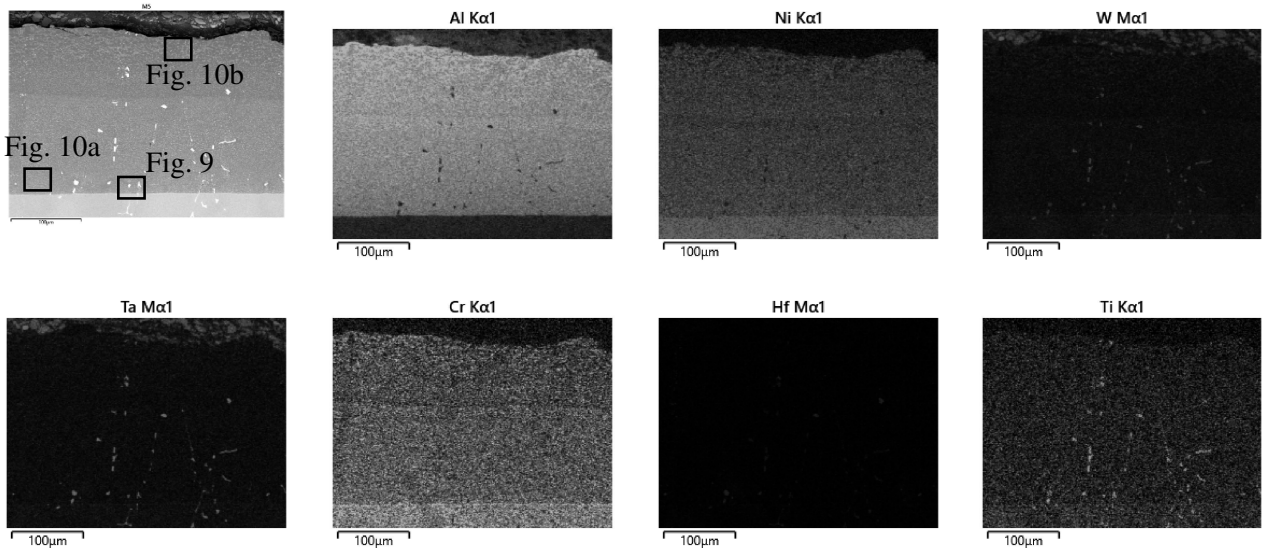

Fig. 8 *Elemental mapping of elements in M5 nickel-based superalloy*

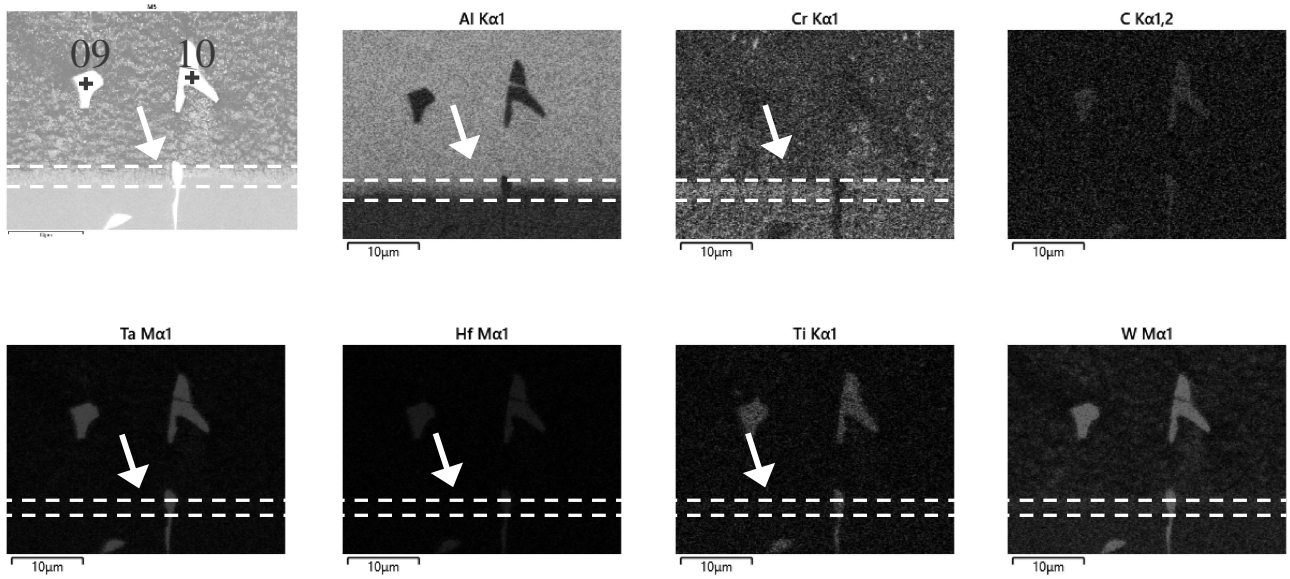

Fig. 9 *Elemental mapping of elements in M5 nickel-based superalloy; Enlarged area of precipitates*

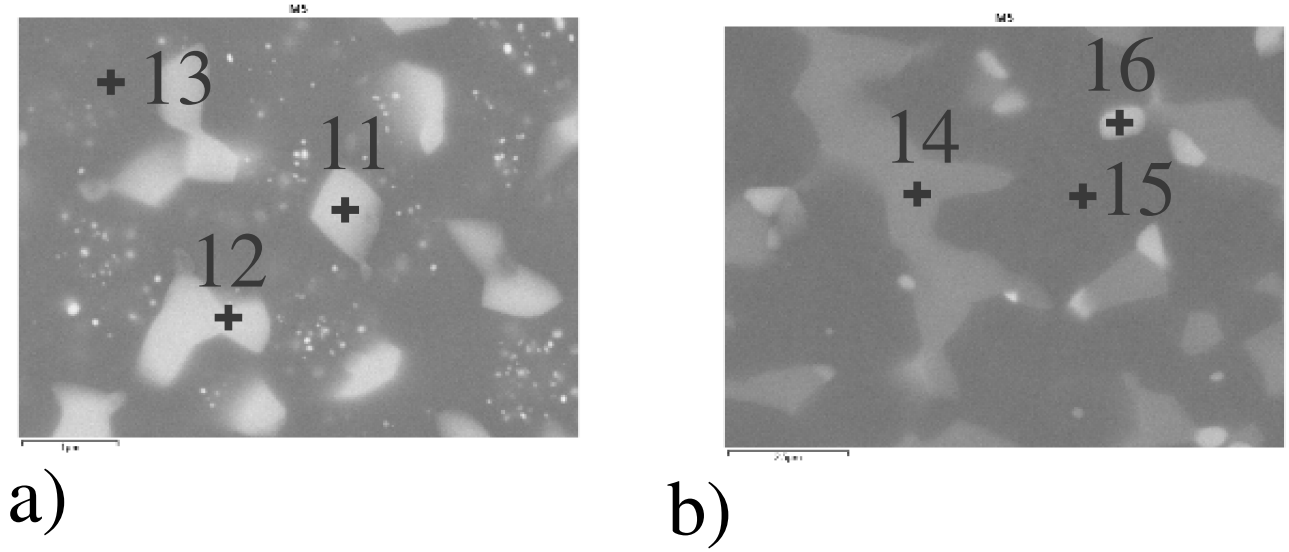

Fig. 10 *Enlarged area of bottom outer zone (a) and upper outer zone (b) in M5 nickel-based superalloy*

Tab. 6 *Point analysis of inclusions presented in Fig. 9, 10*

Spectrum Label	Element content (wt. %)								
	Ni	Al	Co	Cr	Ti	Ta	W	Hf	Mo
09	15.45	4.32	2.79	2.63	7.36	43.19	15.08	8.01	1.17
10	15.73	4.26	2.87	2.79	7.48	42.87	14.78	8.21	1.02
11	33.90	31.55	6.20	7.95	0.52	4.63	14.68	-	0.57
12	27.20	31.05	5.13	10.70	0.50	4.77	20.24	-	0.41
13	44.75	33.03	7.61	3.83	0.38	5.23	5.17	-	-
14	25.03	40.95	4.76	10.69	0.47	1.48	14.64	-	0.28
15	45.42	34.14	6.43	2.78	0.31	6.65	4.19	-	0.09
16	28.10	35.10	4.07	4.77	2.44	11.74	12.61	-	1.17

4 Summary

The comparison of different aluminide coatings produced on Mar M-247 alloy was performed. Samples were aluminized and alumino-silicized for 4 h by two distinct methods. Processes were carried out in special CVD system with various powder mixture composition and process temperature (Tab. 2). Obtained samples were analyzed using SEM microscope with EDX detector. Thickness of aluminide coatings was measured using ImageJ software. Thickness of produced layers varied pronouncedly as an effect of different process conditions. Amount of activator and pure aluminum

had a noticeable effect on the total thickness of obtained layers. Both samples with increased activator and pure aluminum content (M4 and M5) formed 5 to 11.5 x thicker aluminide layers in comparison to M3 sample which was aluminized using a Al-Co powder as aluminum source (Tab. 3, Fig. 1). Thorough microstructural investigations revealed that all coatings comprised outer and inner zone. On the basis of chemical composition and literature findings, identification of some phases as well as most probable reasons of their occurrence was proposed. The outer zone was probably formed by β-NiAl saturated with alloying elements which content is very different for every sample. Chemical composition of several phases found in the upper and bottom part of outer zone was presented (Tab. 6). Further analysis is needed to identify them properly. Inner zone was depleted with Ni and Al. However, clear concentration of: Cr, W, Ta, Hf, Ti was observed as they formed numerous small phases. Big bright phases were scattered throughout the coatings. They comprised strong carbide-formers, so they were probably undissolved MC (M = W, Ta, Ti, Hf) carbides. Co-deposited Si concentrated in outer layer (constant ~3 wt. %) and in big phases located in inner layer (M2 sample). The obtained results were compared with literature findings. Further investigations are needed to specify precise phase composition of analyzed coatings.

References

[1] BASAK A., DAS S., (2016), Carbide Formation in Nickel-Base Superalloy MAR-M247 Processed Through Scanning Laser Epitaxy (SLE) in: *Proceedings of the 27th Annual International Solid Freeform Fabrication Symposium – An Additive Manufacturing Conference*," Austin

[2] JONŠTA P., Vlčková I., JONŠTA Z. (2016). Material Analysis of Nickel Superalloy for Military Technology. In: *Manufacturing Technology*.; vol. 16 no. 2, pp. 348-354. doi: 10.21062/ujep/x.2016/a/1213-2489/MT/16/2/348.

[3] BELAN J, VAŠKO A, KUCHARIKOVÁ L, TILLOVÁ E, CHALUPOVÁ M. (2019), The SEM Metallography Analysis of Vacuum Cast ZhS6K Superalloy Turbine Blade after Various Working Hours. In: *Manufacturing Technology*.; vol. 19, iss. 5, pp. 727-733. doi: 10.21062/ujep/362.2019/a/1213-2489/MT/19/5/727

[4] ALPERINE S., STEINMETZ P., JOSSO P. COSTANTINI A., (1989), High Temperature-resistant Palladium-modified Aluminide Coatings for Nickel-base Superalloys in: *Materials Science and Engineering,* vol. A121, pp. 367-372, https://doi.org/10.1016/0921-5093(89)90789-2

[5] RHYS-JONES T. N., (1989), Coatings for blade and vane applications in gas turbines, in: *Corrosion Science,* vol. 29, no. 6, pp. 623-646, https://doi.org/10.1016/0010-938X(89)90104-2

[6] THOMA M., SCRIVANI A., GIOLLI C. GIORGETTI A., (2011), Aluminizing Turbine Parts: Processes and Coatings In:*Proceedings of ASME Turbo Expo 2011*, Paper No: GT2011-46843, pp. 783-789; https://doi.org/10.1115/GT2011-46843

[7] KHAJAVI M. R., SHARIAT M. H., PASHA A.,(2004), Aluminide Coatings for Nickel Based Superalloys, In: *Surface Engineering,* vol. 20, no. 4, pp. 261-265, https://doi.org/10.1179/026708404X4672

[8] KRBATA, M.; FABO, P.; KOHUTIAR, M.; ESCHEROVA, J.; KUBA, M.; KIANICOVA, M.; ECKERT, M., (2023) Possibilities of Using Impedance Spectroscopy for Indirect Measurements of Thin Layers of Al & Cr-Al Coatings on Ni-based Superalloy Inconel 713LC Applied by the "Out-of-pack" Diffusion Method. In: *Manufacturing Technology*, vol. 23 (3), 313-318.

[9] PATNAIK P. C., (1989) Intermetallic Coatings for High Temperature Applications – A Review, In: *Materials and Manufacturing Processes*, vol. 4:1, pp. 133-152 https://doi.org/10.1080/10426918908956276

[10] SIVAKUMAR R., MORDIKE B. L., (1989), High temperature coatings for gas turbine blades: A review In: *Surface and Coatings Technology,* vol. 37, Issue 2 pp. 139-160, https://doi.org/10.1016/0257-8972(89)90099-6

[11] GOWARD G. W., BOONE D. H., (1971), Mechanisms of Formation of Diffusion Aluminide Coatings on Nickel-Base Superalloys In: *Oxidation of Metals,,* vol. 3, no. 5, pp. 475-495, https://doi.org/10.1007/BF00604047

[12] HAN, X. (2011)*Diffusion Coatings for High-Temperature Applications on Ni-base Superalloys,* PhD Desideration, Milano: Politecnico di Milano, Department of Mechanical Engineering,

[13] TAMARIN Y. (2002) Protective Coatings for turbine Blades, Ohio: ASM International

[14] BIANCO R., RAPP R. A., (1996), Pack cementation diffusion coatings In: *Metallurgical and Ceramic Protective Coatings*, London, Chapman and Hall, pp. 236-260, DOI: 10.1007/978-94-009-1501-5_9

[15] MEVREL R., DURET C. PICHOIR R., (1986),Pack Cementation processes In: *Materials Science and Technology ,* vol. 2, Issue 3, pp. 201-207, https://doi.org/10.1179/mst.1986.2.3.201

[16] GOWARD G. W., CANNON L. W., (1988), Pack Cementation Coatings for Superalloys: a Review of History, Theory, and Practice In: *Journal of Engineering for Gas Turbines and Power,* vol. 110, pp. 150-154, https://doi.org/10.1115/1.3240078

[17] GÓRAL M., OCHAŁ K., KUBASZEK T. DRAJEWICZ M. (2020), The influence of deposition technique of aluminide coatings on oxidation resistance of different nickel superalloys, In: *Materials Today: Proceedings,* no. 33, part 4, pp. 1746-1751, https://doi.org/10.1016/j.matpr.2020.04.863

[18] ROMANOWSKA J., DRYZEK E., MORGIEL J., SIEMEK K., KOLEK Ł., ZAGUŁA-YAVORSKA M., (2018) Microstructure and positron lifetimes of zirconium modified aluminide coatings In: *Archives of Civil and Mechanical Engineering,* vol. 18, pp. 1150-1155, https://doi.org/10.1016/j.acme.2018.03.002

[19] PYTEL M., GÓRAL M. MALINIAK M., (2012), The influence of production method on oxidation resistance of the aluminide coatings obtained on IN 100 alloy, In: *Archives of materials Science and Engineering,* vol. 2, pp. 102-108,

[20] SWADZBA L., NAWRAT G., MENDALA B. GORAL M., (2011), The influence of deposition process on structure of platinum-modifed aluminide coatings on Ni-base superalloy In: *Key Engineering Materials,* no. 465, pp. 247-250, https://doi.org/10.4028/www.scientific.net/KEM.465.247

[21] GORAL M., PYTEL M., OCHAL K., DRAJEWICZ M., KUBASZEK T., (2021) "Microstructure of aluminide coatings modified by Pt, Pd, Zr and Hf formed in low-activity CVD process In: *Coatings,* vol. 11, no. 4, p. 421, https://doi.org/10.3390/coatings11040421

[22] SITEK R., BOLEK T., DOBOSZ R., PLOCINSKI T., MIZERA J., (2016) Microstructure and oxidation resistance of aluminide layer produced on Inconel 100 nickel alloy by CVD method In: *Surface and Coatings Technology,* vol. 304, pp. 584-591, https://doi.org/10.1016/j.surfcoat.2016.07.072

[23] SIENKIEWICZ J., SITEK R., URA-BIŃCZYK E., KURZYDŁOWSKI K. J., (2011) "Mikrostruktura i odporność korozyjna dyfuzyjnych warstw aluminidkowych wytworzonych na podłożu nadstopu niklu Inconel 713V In *Proceedings* of XXXIX Szkoła inżynierii Materiałowej, Kraków-Krynica

[24] BOZZA F., BOLELLI G., GIOLLI C., GIORGETTI A., LUSVARGHI L., SASSATELLI P., SCRIVANI A., CANDELI A. THOMA M., (2014), Diffusion mechanisms and microstructure development in pack aluminizing of Ni-based alloys In: *Surface and Coatings Technology,* vol. 239, pp. 147-159, https://doi.org/10.1016/j.surfcoat.2013.11.034

[25] NASH P., SINGLETON M. F. MURRAY J. L., (2010) Desk Handbook: Phase Diagrams of Binary Nickel Aloys, Second Edition, Ohio: ASM International, ISBN: 978-0-87170-403-0

[26] MUTASIM Z., KIMMEL J., BRENTNALL W., (1998) Effects of Alloy Composition on the Performance of Diffusion Aluminide Coatings, In: Proceedings *ASME 1998 International Gas Turbine and Aeroengine Congress and Exhibition,* vol. 345, pp. 1-6, https://doi.org/10.1115/98-GT-401

[27] MILENKOVIC S., SABIROV I., LLORCA J., (2012), Effect of the cooling rate on microstructure and hardness of MAR-M247 Ni-based superalloy, In: *Materials Letters,* vol. 73, pp. 216-219, https://doi.org/10.1016/j.matlet.2012.01.028

[28] WAWRO S. W. (1982) MC carbide structures in Mar-M247, *NASA Report 167892* (Lewis Research)

[29] Baldan R., Pereirada Rocha R. L., Tomasiello R. B., Nunes C. A., Silva Costa A. M., Ribeiro M. J. Barboza, Coelho G. C., Rosenthal R., (2013),Solutioning and Aging of MAR-M247 Nickel-Based Superalloy In: *Journal of Materials Engineering and Performance,* vol. 22, no. 9, pp. 2574-2579,

[30] PATNAIK P. C. IMMARIGEON J. P. (1989) Protective Coatings For Aero Engine Hot Section Components In: *Materials and*

Manufacturing Processes, vol. 4, no. 3, pp. 347-384, https://doi.org/10.1080/10426918908956299

[31] BIANCO R., RAPP R. A., (1993) Pack Cementation Aluminide Coatings on Superalloys: Codeposition of Cr and Reactive Elements In: *Journal of Electrochemical Society,* vol. 140, no. 4, pp 1181, DOI 10.1149/1.2056219

[32] WU Q., YANG R.-B., WU Y.-X., S.-S. LI, MA Y., GONG S.-K., (2011), A comparative study of four modified Al coatings on Ni_3Al-based single crystal superalloy In: *Progress in Natural Science: Materials International,* vol. 21, pp. 496-505, https://doi.org/10.1016/S1002-0071(12)60089-6

[33] BOSE S., (2002), *High temperature coatings*, Burlington: Butterworth Heinemann, ISBN: 9780080469553

[34] STRANDLUND H. LARSSON H., (2004) Prediction of Kirkendall shift and porosity in binary and ternary diffusion couples In: *Acta Materialia,* vol. 52, Issue 15, pp. 4695-4703, DOI: 10.1016/j.actamat.2004.06.039

[35] YAVORSKA M., ZIELIŃSKA M., KUBIAK K., SIENIAWSKI J., (2010) Mikrostruktura i odporność na utlenianie izotermiczne powłoki aluminidkowej wytworzonej w niskoaltywnym procesie CVD na podłożu stopu Inconel 713 LC In *Archiwum Technologii Maszyn i Automatyzacji,* vol. 30, no. 1, pp. 83-94, 2010.

[36] THOMA M., MORANT M., (1996) Slurry Coating Systems for Low and High Temperature Turbine Protection: New Developments in *Proceedings of ASME 1996 Turbo Asia Conference* ISBN:978-0-7918-7877-4, Paper No: 96-TA-056, V001T07A006, https://doi.org/10.1115/96-TA-056

[37] TIAN W. H., HAN C. S. NEMOTO M., (1999) Precipitation of α-Cr in B2-ordered NiAl In: *Intermetallics,* vol. 7, Issue 1, pp. 59-67, https://doi.org/10.1016/S0966-9795(98)00015-6

[38] TU X., PENG H., ZHENG L., QI W., HE J., GUO H., GONG S., Oxidation and microstructure evolution of Al–Si coated Ni_3Al based single crystal superalloy with high Mo content In: *Applied Surface Science,* vol. 325, pp. 20-26, https://doi.org/10.1016/j.apsusc.2014.11.076

[39] SZCZOTOK A., RODAK K., (2012) Microstructural studies of carbides in MAR-M247 nickel-based superalloy In: *Materials Science and Engineering*, vol. 35, pp. 1–11

[40] KAUFMAN M., (1984), "Properties of Cast Mar-M-247 for Turbine Blisk Applications In: *Materials Science,* pp. 43-52,

[41] SZCZOTOK A. (2011), Quantitative evaluation of carbides in nickel-base superalloy MAR-M247 In: *Materials Science and Engineering,* vol. 22, pp. 1-11, doi:10.1088/1757-899X/22/1/012007

[42] JONŠTA P., VLČKOVÁ I., JONŠTA Z., PODHORNÁ B., (2015), Materialographic Analysis of MAR M-247 Superalloy In: *Key Engineering Materials,* vol. 647, pp. 66-71, https://doi.org/10.4028/www.scientific.net/KEM.647.66

[43] ESLAMI A., ARABI H., RASTEGARI S., (2009) Gas Phase Aluminizing of a Nickel Base Superalloy by a Single Step HTHA Aluminizing Process In: *Canadian Metallurgical Quarterly,* vol. 48, no. 1, pp. 91-98, DOI: 10.1179/000844309794239215

[44] SINGH, K. (2014), Advanced Materials for Land Based Gas Turbines, In: *Transactions of the Indian Institute of Metals,* vol. 67, no. 5, pp. 601-615, DOI: 10.1007/s12666-014-0398-3